Polarization patterns of thick clouds: overcast skies have distribution of the angle of polarization similar to that of clear skies

Ramón Hegedüs,[1] Susanne Åkesson,[2] and Gábor Horváth[1],*

[1]*Biooptics Laboratory, Department of Biological Physics, Physical Institute, Eötvös University, H-1117 Budapest, Pázmány sétány 1, Hungary*
[2]*Department of Animal Ecology, Lund University, Ecology Building, SE-223 62 Lund, Sweden*
Corresponding author: gh@arago.elte.hu

The distribution of polarization in the overcast sky has been practically unknown. Earlier the polarization of light from heavily overcast skies (when the Sun's disc was invisible) has been measured only sporadically in some celestial points by point-source polarimetry. What kind of patterns of the degree p and angle α of linear polarization of light could develop after transmission through a thick layer of ice or water clouds? To answer this question, we measured the p and α patterns of numerous totally overcast skies on the Arctic Ocean and in Hungary by full-sky imaging polarimetry. We present here our finding that depending on the optical thickness of the cloud layer, the pattern of α of light transmitted through the ice or water clouds of totally overcast skies is qualitatively the same as the α pattern of the clear sky. Under overcast conditions the value of α is determined predominantly by scattering on cloud particles themselves. Nevertheless, the degrees of linear polarization of light from overcast skies were rather low ($p \leq 16\%$). Our results obtained under overcast conditions complete the earlier findings that the α pattern of the clear sky also appears in partly cloudy, foggy, and smoky skies. Our results show that the celestial distribution of the direction of polarization is a very robust pattern being qualitatively always the same under all possible sky conditions. This is of great importance for the orientation of polarization-sensitive animals based on sky polarization under conditions when the Sun is not visible. © 2007 Optical Society of America

OCIS codes: 010.1290, 110.2960, 120.5410, 280.1310, 330.7310.

1. INTRODUCTION

The mathematical and physical description of the state of polarization of sunlight scattered in and transmitted through the Earth's atmosphere is a difficult problem. Thus the theoretical calculations and computer simulations of the atmospheric radiative transfer concentrated mainly on the polarization characteristics of the clear sky [1]. The polarimetric measurements partly compensated this one-sided approach by gathering polarization data not only from clear skies but also from turbid ones polluted by aerosol, smoke, dust, and smog, for instance [1]. These earlier measurements were performed by point-source polarimetry, which limited the number of celestial points at which information on skylight polarization could be collected. Due to this technical limitation and the difficulty of theoretical and computational study of the polarization of non-clear skies, the polarimetry of cloudy, smoky, foggy, and overcast skies has been neglected.

A breakthrough of the mentioned technical limitation has happened by the development of full-sky imaging polarimeters, which made it possible to take simultaneous measurement of skylight polarization in huge numbers of celestial points [2–4]. Due to full-sky imaging polarimetry, it became possible to measure the polarization patterns of partly cloudy [5,6], foggy [7], and smoky [8] skies. However, until now an experimental study of the polarization patterns of overcast skies remained a debt of atmospheric polarimetry.

The distribution of polarization in the overcast sky has been practically unknown [1,9,10]. Although Coulson [11] measured the degree of linear polarization $p = \sqrt{Q^2 + U^2}/I$ of skylight (where I, Q, and U are the first three components of the Stokes vector) under conditions of a heavy stratus overcast along the solar and antisolar meridians at five different solar elevations, these data were gathered only from a few celestial points by point-source polarimetry. According to Coulson [11], p of light from the overcast sky is extremely low ($p < 2.5\%$). Unfortunately, he did not publish data on the angle of polarization $\alpha = 0.5 \times \arctan(U/Q)$ of light from the overcast sky. Using a point-source polarimeter, Brines and Gould [12] also measured the polarization of light from the overcast sky when the Sun's disc was invisible. Since they obtained extremely low p values and directions of polarization diverging considerably from the theoretical predictions, they expected that only in exceptional circumstances would the polarization patterns produced in the atmosphere above the clouds be transmitted through even relatively thin sections of cloud cover.

On the one hand, it could be assumed that α of light from an overcast sky changes randomly in space and time due to the strong multiple scattering on cloud particles

(water droplets or ice crystals), the density of which changes spatiotemporally in a chaotic manner. On the other hand, however, if the cloudlight is not unpolarized ($p \neq 0$), one could expect that a certain (unknown) non-random pattern of the angle of polarization α of skylight could develop after transmission through the thick cloud layer of the overcast sky. As far as we know, 180° field-of-view p and α patterns of overcast skies have not been measured until now. This information would also be important for researchers studying the orientation of polarization-sensitive animals based on sky polarization.

Therefore we measured the polarization patterns of numerous totally overcast skies on the Arctic Ocean and in Hungary by full-sky imaging polarimetry in the red, green, and blue parts of the spectrum. We present here our finding that depending on the optical thickness of the cloud layer, the α pattern of totally overcast skies is similar to that of clear skies. Our results obtained under overcast conditions complete the earlier findings that the α pattern of the clear sky occurs also in partly cloudy [5,6], foggy [7], and smoky [8] skies. The importance of this feature of sky polarization for the orientation of polarization-sensitive animals is briefly discussed.

2. MATERIALS AND METHODS

The polarization patterns of clear and totally overcast skies were measured at two different geographical re-

gions: (1) Between 25 August and 11 September 2005 at different locations during the third part of the international Arctic polar research expedition "Beringia 2005," organized by the Swedish Polar Research Secretariat. The expedition crossed the Arctic Ocean with the Swedish icebreaker Oden departing from Barrow in Alaska (71°17′ N, 156°47′ W) and arriving in Longyearbyen (78°12′N, 15°49′ E) on the island of Spitsbergen (Svalbard, Norway). (2) Between 14 February and 17 March 2006 in the vicinity of the Hungarian town Göd (47°70′ N, 19°15′ E) on the shore of Danube River. The date, time, geographical coordinates (latitude, longitude), weather, and surface conditions (snowing or raining, occurence of snow cover on the terrain) during the measurements are summarized in Table 1. During the measurements the Sun was always invisible to the human observer due to the heavy overcast. The solar elevation angle ϵ from the horizon was determined from the exact time and geographical coordinates (Table 1) of the place of measurements using the online solar position calculator of the U.S. Naval Observatory, Astronomical Applications Department (http://aa.usno.navy.mil). The composition (ice crystals or water droplets) of clouds of the overcast sky was confirmed only if it was snowing or raining during the measurements.

The skylight polarization was measured by full-sky imaging polarimetry, the technique and evaluation proce-

Table 1. Date, Time, Geographical Coordinates, Solar Elevation Angle, and Weather and Surface Conditions during Full-Sky Imaging Polarimetric Measurements Performed in the High Arctic (Skies S0–S8) and Hungary (S9–S15)[a,b]

Sky No.	Date	Time	Latitude	Longitude	Solar Elevation	Weather and Surface Conditions
				Arctic (ice/snow cover of the Arctic Ocean)		
	2005	UTC−8				
S0	25 Aug.	21:20	78°27.8′ N	149°9.1′ W	6.3°	clear, cloudless sky, snow cover
S1	26 Aug.	21:00	79°27.7′ N	144°54.7′ W	6.1°	overcast, snowing → ice clouds, snow cover
S2	26 Aug.	21:35	79°27.7′ N	144°54.7′ W	4.6°	overcast, snowing → ice clouds, snow cover
S3	26 Aug.	22:35	79°27.7′ N	144°54.7′ W	2.3°	overcast, snowing → ice clouds, snow cover
S4	28 Aug.	20:45	80°53.7′ N	145°36.3′ W	6.9°	overcast, snow cover
S5	4 Sep.	21:10	86°38.7′ N	174°38.6′ E	7.3°	overcast, snow cover
S6	6 Sep.	20:43	87°39.1′ N	151°15.3′ E	5.7°	overcast, snow cover
S7	6 Sep.	22:37	87°39.1′ N	151°15.3′ E	4.7°	overcast, snowing → ice clouds, snow cover
S8	11 Sep.	05:00	89°15.5′ N	172°22.6′ W	3.9°	overcast, snow cover
				Hungary (Göd town)		
	2006	UTC+1				
S9	14 Feb.	17:00			0.4°	overcast, snow cover
S10	16 Feb.	12:17			29.9°	overcast, snowing → ice clouds, snow cover
S11	16 Feb.	16:03			9.2°	overcast, snowing → ice clouds, snow cover
S12	17 Feb.	16:25	47°42′N	19°9′E	6.2°	overcast, raining → water clouds, snow cover
S13	25 Feb.	12:14			33.1°	overcast, snow cover
S14	15 Mar.	16:32			11.9°	overcast, dark terrain
S15	17 Mar.	16:15			15.1°	overcast, raining→ water clouds, dark terrain

[a]S0, clear sky; S1–S15, totally overcast sky

[b]In the Arctic the substratum was the high-albedo (white) ice/snow cover. In Hungary in most cases the terrain was covered by high-albedo (white) snow, but from March 15, 2006, the snow cover disappeared, and thus the albedo of the dark terrain without vegetation became low. When it was snowing or raining, the clouds of the overcast sky were obviously composed of ice crystals and water droplets, respectively; otherwise the composition of the clouds was unknown.

dure of which have been described in detail elsewhere [4]. A 180° field of view (full sky) was ensured by a fisheye lens (Nikon-Nikkor, $F=2.8$, focal length 8 mm) with a built-in rotating disc mounted with three broadband (275–750 nm) neutral density linearly polarizing filters (Polaroid HNP′B) with three different polarization axes (0°, 45°, and 90° from the radius of the disc). The detector was a photo emulsion (Kodak Elite Chrome ED 200 ASA color reversal film; the maxima and half-bandwidths of its spectral sensitivity curves were $\lambda_{red}=650\pm40$ nm, $\lambda_{green}=550\pm40$ nm, $\lambda_{blue}=450\pm40$ nm) in a roll-film photographic camera (Nikon F801). For a given sky three photographs were taken for the three different directions of the transmission axis of the polarizers. The camera was set on a tripod such that the optical axis of the fisheye lens was vertical, i.e., pointed to the zenith. After 24-bit (3×8 for red, green, and blue) digitization (by a Canon Arcus 1200 scanner) of the three chemically developed color pictures for a given sky and their computer evaluation, the patterns of the radiance I, degree of linear polarization p, and angle of polarization α (measured clockwise from the local meridian) of skylight were determined as color-coded two-dimensional circular maps, in which the center is the zenith, the perimeter is the horizon, and the zenith angle θ is proportional to the radius from the zenith (zenith: $\theta=0°$, horizon: $\theta=90°$). These patterns were obtained in the red, green, and blue spectral ranges, in which the three color-sensitive layers of the photo emulsion used have maximal sensitivity. The degree p and

angle α of linear polarization were measured by our polarimeter with an accuracy of $\Delta p=\pm1\%$ and $\Delta\alpha=\pm2°$, respectively.

The noisiness n of a given α pattern (Table 2) was calculated as follows: the α patterns were scanned throughout with a window of 5×5 pixels, in which the standard variance (σ^2) of the angle of polarization α was calculated and then the average of the standard variances of all 5×5-pixel windows was obtained. Finally, this value was normalized to that of white noise calculated with the same method. Thus, noisiness n of an α pattern denotes how noisy it is compared with the white noise (no noise: $n=0\%$, white noise: $n=100\%$).

3. RESULTS

We measured the patterns of the radiance I, degree of linear polarization p, and angle of polarization α (clockwise from the local meridian) of a clear Arctic sky (number S0) above the extended ice/snow cover of the Arctic Ocean by full-sky imaging polarimetry in the red (650 nm), green (550 nm), and blue (450 nm) parts of the spectrum (Fig. 1). As expected, I of the light from the clear sky (Fig. 1A) was highest in the blue and lowest in the red spectral range (Figs. 1B–1D, Table 2). p of light from the clear sky was highest at 90° from the Sun and gradually decreased toward the solar and antisolar points (Figs. 1E–1G); furthermore, p was highest in the red ($p_{max}=59\%$) and low-

Table 2. Optical Characteristics of Clear and Totally Overcast Skies Measured by Full-Sky Imaging Polarimetry in the Red (650 nm), Green (550 nm), and Blue (450 nm) Parts of the Spectrum[a]

Sky No.	Relative Radiance $i(\%)$			Degree of Linear Polarization $p(\%)$			Noisiness $n(\%)$ of Angle of Polarization α		
	Red	Green	Blue	Red	Green	Blue	Red	Green	Blue
Arctic Clear Sky									
S0	46 ± 17	52 ± 16	74 ± 13	34 ± 25	25 ± 16	21 ± 15	5	3	6
Arctic Totally Overcast Skies									
S1	51 ± 7	44 ± 5	62 ± 6	6 ± 4	5 ± 3	4 ± 3	32	43	30
S2	63 ± 5	54 ± 4	82 ± 4	5 ± 3	5 ± 3	4 ± 2	28	29	24
S3	57 ± 5	46 ± 3	66 ± 4	5 ± 4	5 ± 3	4 ± 3	33	41	30
S4	57 ± 5	48 ± 4	72 ± 4	5 ± 4	5 ± 3	4 ± 3	31	34	27
S5	63 ± 5	53 ± 3	66 ± 3	5 ± 3	5 ± 3	4 ± 2	28	38	29
S6	45 ± 3	41 ± 2	59 ± 2	7 ± 4	7 ± 4	5 ± 3	36	37	23
S7	43 ± 4	38 ± 3	55 ± 3	8 ± 5	8 ± 5	6 ± 3	30	40	22
S8	59 ± 7	53 ± 6	82 ± 7	5 ± 3	4 ± 3	3 ± 2	27	33	31
Hungarian Totally Overcast Skies									
S9	57 ± 9	45 ± 8	74 ± 13	5 ± 3	5 ± 3	4 ± 3	27	38	29
S10	70 ± 8	52 ± 6	73 ± 9	5 ± 3	5 ± 3	5 ± 3	29	42	31
S11	60 ± 9	49 ± 8	74 ± 12	5 ± 3	5 ± 3	4 ± 3	26	32	28
S12	67 ± 5	57 ± 5	77 ± 4	4 ± 3	4 ± 3	3 ± 2	27	32	32
S13	73 ± 10	56 ± 9	77 ± 12	5 ± 3	5 ± 3	5 ± 3	26	36	29
S14	64 ± 8	56 ± 8	73 ± 9	3 ± 3	4 ± 3	3 ± 2	28	30	23
S15	71 ± 15	52 ± 11	77 ± 16	5 ± 3	6 ± 4	5 ± 3	30	42	39

[a]The radiance I is normalized to the highest value I_{max}, resulting in the relative radiance $i=I/I_{max}$ (average ± standard deviation). The degree of linear polarization p (average ± standard deviation) is averaged over the entire sky. The noisiness n of the angle of polarization α is computed for the whole sky as described in Section 2. The date, time, latitude, longitude, and weather and surface conditions during the measurements are given in Table 1.
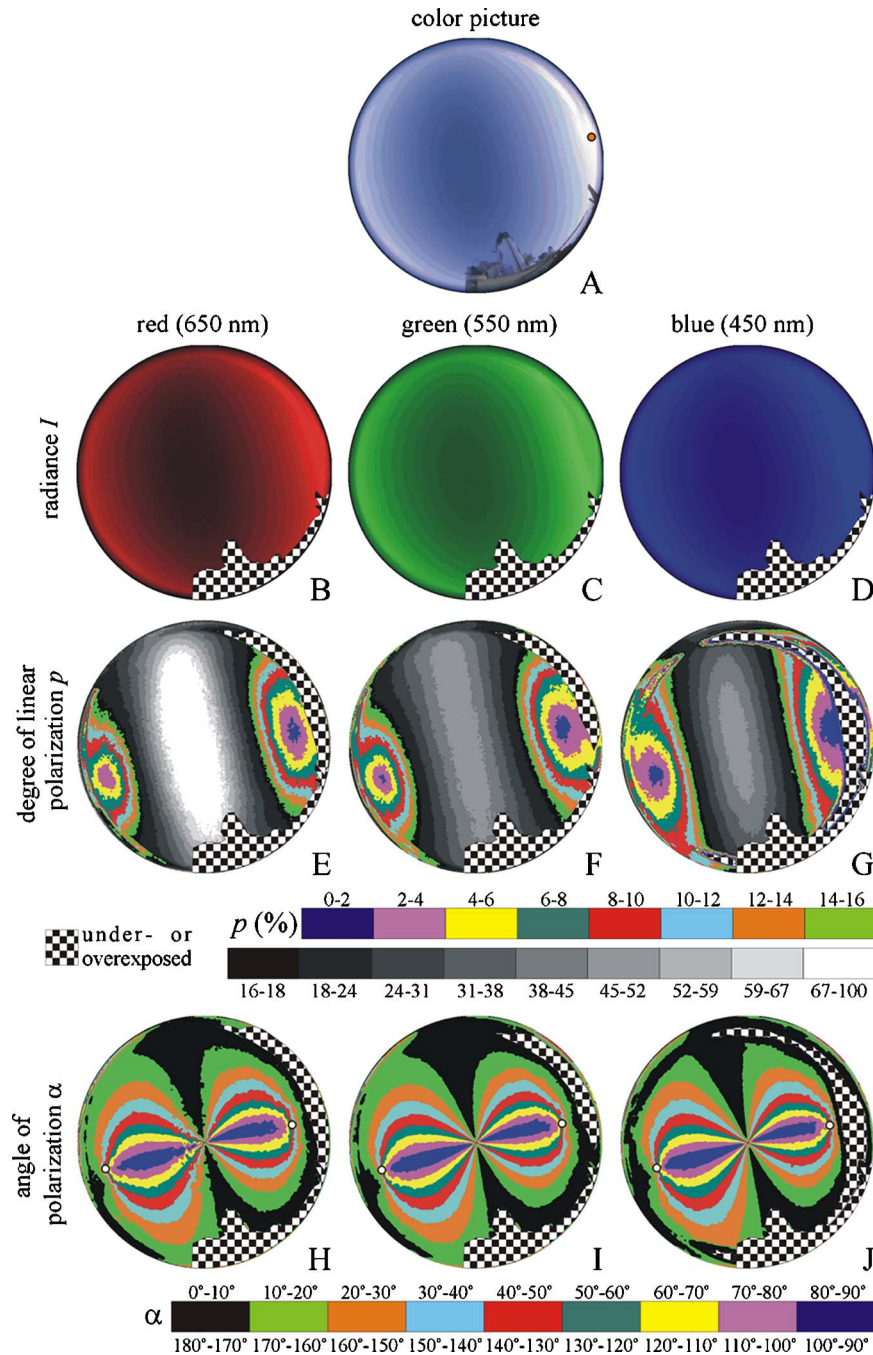
Fig. 1.   (Color online) Color picture (A) and patterns of the radiance I (B–D), degree of linear polarization p (E–G), and angle of polarization α measured clockwise from the local meridian (H–J) of the Arctic clear sky S0 (Table 1) measured by full-sky imaging polarimetry in the red (650 nm), green (550 nm), and blue (450 nm) parts of the spectrum. The optical data of this sky are given in Table 2. The optical axis of the fisheye lens was vertical; thus the horizon is the perimeter and the center of the circular patterns is the zenith. On the bottom of the circular color picture the silhouette of the Swedish icebreaker Oden can be seen. In A the position of the sun near the horizon is marked by a gray dot (orange online) and in the α patterns (H–J) the positions of the Arago and Babinet neutral (unpolarized) points are marked by white dots with black perimeters.

est in the blue ($p_{max}=36\%$) part of the spectrum (Table 2). The angle of polarization α of light from the clear sky had a characteristic pattern (Figs. 1H–1J): the isolines with α=constant were always eight shaped with a center at the zenith and an axis of mirror symmetry coinciding with the solar–antisolar meridian in such a way that the smaller loop of the eight figure was always in the solar half of the sky. In Figs. 1H–1J the different intervals of α

are shaded by various colors (red, for example, codes the intervals $40° \leq \alpha \leq 50°$ and $130° \leq \alpha \leq 140°$). We measured the I, p, and α patterns of numerous other clear Arctic and Hungarian skies and obtained the same optical characteristics as described above.

We measured the I, p, and α patterns of a totally overcast sky (number S9) in Hungary over an extended snow surface in the red, green, and blue spectral ranges (Fig.

2). The radiance I of light from the overcast sky (Fig. 2A) was highest in the blue and lowest in the green spectral range (Figs. 2B–2D, Table 2). The degree of linear polarization p of light from the overcast sky was very low, and its pattern had approximately a rotational symmetry with a minimum near the zenith and an approximately annular maximum on the horizon (Figs. 2E–2G). Depending on the wavelength, the maximum of p ranged between 4% and 16%. These characteristics of the I and p patterns are also true for all other overcast skies S1–S15 investigated (Table 2).

To our surprise the patterns of the angle of polarization α of the overcast sky S9 (Figs. 2H–2J) were qualitatively

the same as those of the clear sky S0 (Figs. 1H-1J): at all three (red, green, and blue) spectral ranges the α isolines were again eight shaped with a center at the zenith and a symmetry axis along the solar–antisolar meridian. This is also true for all other overcast skies S1–S15 studied (Fig. 3). Although Fig. 3 shows only the α patterns of overcast skies measured in the blue spectral range, quite similar α patterns were obtained also in the green and red parts of the spectrum.

Due to the strong multiple scattering of light on the cloud particles (ice crystals or water droplets) the degree of linear polarization p of light from the overcast sky was considerably reduced in comparison with p of light from
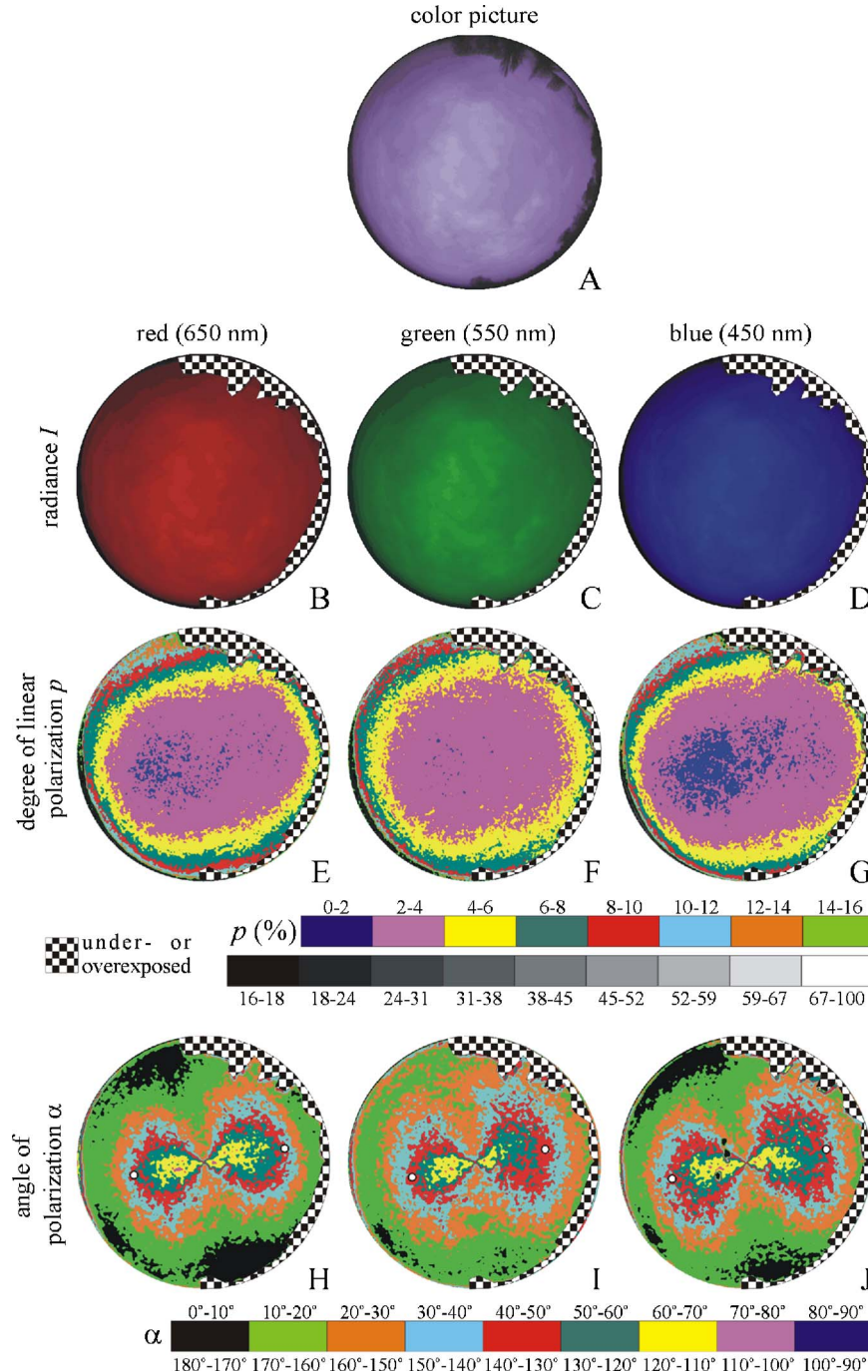

Fig. 2. (Color online) Same as Fig. 1 but for the totally overcast sky S9, the data of which are given in Tables 1 and 2. On the periphery of the color picture the dark silhouette of some trees can be seen.
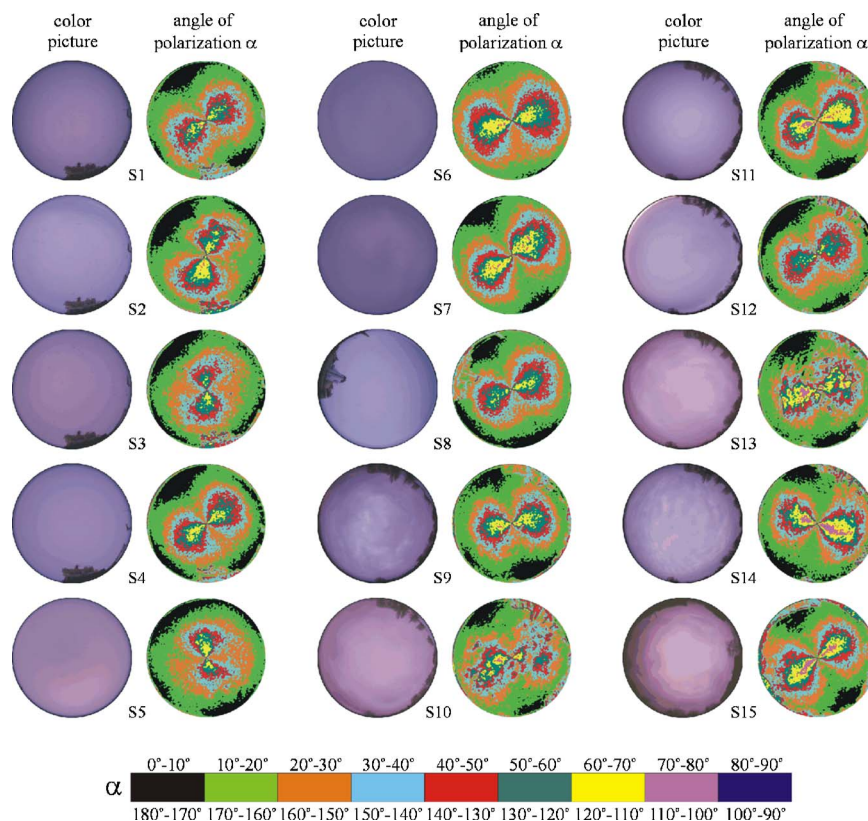
Fig. 3.   (Color online) Color pictures and patterns of the angle of polarization α (measured clockwise from the local meridian) of Arctic and Hungarian total overcast skies S1–S15, the data of which are given in Tables 1 and 2. The α patterns were measured by full-sky imaging polarimetry in the blue (450 nm) part of the spectrum. Quite similar α patterns were obtained in both the green and red spectral ranges.

the clear sky (Table 2); furthermore, the α pattern of the overcast sky was noisier than that of the clear sky. The noisiness $(22\% \le n \le 43\%)$ of the overcast skies S1–S15 was about seven times higher than that of the clear sky S0 $(3\% \le n \le 6\%)$. Interestingly, the noisiness n of overcast skies was highest in the green spectral range (Table 2), the reason of which is unknown. Based on these findings we conclude that depending on the optical thickness of the ice or water clouds (Table 1) and the wavelength, the α pattern of totally overcast skies is similar to that of the clear sky.

At low solar elevations (when the elevation angle ϵ of the sun from the horizon is not larger than about 25°), there are always two unpolarized (neutral) points in the clear sky: the Babinet point above the Sun and the Arago point above the anti-Sun. Both neutral points are placed along the solar and antisolar meridians at a position where the negative polarization of skylight (characterized by angles of polarization $-45° \le \alpha \le +45°$ measured from the local meridian) switches to positive polarization (characterized by $+45° \le \alpha \le +135°$). The Arago and Babinet neutral points are placed at the intersections of the solar–antisolar meridian and the so-called neutral line. The latter is a line along which $\alpha = +45°$ or $+135°$. The solar elevation angle ϵ from the horizon was between 0° and 33.1° for the skies S0–S15 studied (Table 1).

In Figs. 1H–1J the neutral line of the α patterns of the clear sky S0 runs within the red eight-shaped region characterized by $+41° \le \alpha \le +50°$ and $131° \le \alpha \le +140°$,

and the positions of the Arago and Babinet points are marked by small circles. According to our measurements, the zenith angles of the Arago and Babinet points of the clear sky decreased with decreasing wavelength (i.e., the neutral points were closer to the zenith in the blue part of the spectrum than in the red part). The consequence of this dispersion (i.e., wavelength dependency) is that the regions of negative polarization around the Sun and anti-Sun in the clear sky are larger at the shorter wavelengths than at the longer ones. In Figs. 2H–2J the Arago and Babinet neutral points occur again in the α patterns of the overcast sky S9. The same is true also for all investigated overcast skies S1–S15. Note, however, that in Fig. 3 the positions of the Arago and Babinet neutral points are not displayed. The wavelength dependency of the position of the neutral points was weaker for the overcast skies than for the clear skies.

4. DISCUSSION

A. Atmospheric Optical Consequences

As the unpolarized sunlight enters the Earth's atmosphere, it is Rayleigh-scattered by air, the consequence of which is that it becomes partially linearly polarized. If the atmosphere is clear (cloudless), this scattering phenomenon results in the well-known spatial distribution of the radiance I and color c (e.g., the ratio of radiances of skylight at two different wavelengths) as well as the degree p and angle α of linear polarization of the sky (Fig. 1). In

the past these I, c, p, and α patterns of the clear sky were thoroughly studied theoretically as well as experimentally, because the understanding of these optical characteristics of the clear blue sky was one of the most interesting and important problems in atmospheric optics [1,9,10,13,14].

To our knowledge, Coulson [11] and Brines and Gould [12] were the only researchers who performed preliminary experimental studies of the polarization of light from the overcast sky. Coulson [11] measured the degree of linear polarization p of skylight in Los Angeles under conditions of a heavy and persistent overcast of stratus clouds at 652 nm in several points of the solar and antisolar meridians at five different solar elevation angles: $\epsilon=$ $-2.4°, 3.5°, 14.8°, 47.5°, 54.8°$. He obtained that p was not higher than 2.5% at $\epsilon=-2.4°, 3.5°, 14.8°, 47.5°$, and the maximum of p reached only 10% at $\epsilon=54.8°$, when the stratus clouds started to break up with decreasing thickness. The radiance of cloudlight was essentially independent of azimuth, with a gradual decrease from zenith to horizon and the zenith being two to three times as bright as the horizon. These results of Coulson [11] are corroborated by our results obtained by full-sky imaging polarimetry and presented here. Brines and Gould [12] experienced that when the sky was completely overcast (Sun's disc invisible) p decreased from the horizon toward the zenith, its maximum was only 3%, and the angle of polarization α diverged greatly from the single-scattering Rayleigh expectations.

In this work we completed the pioneering point-source polarimetric measurements of Coulson [11] and Brines and Gould [12] on the polarization of the overcast sky with the use of full-sky imaging polarimetry. We found that not only the pattern of the radiance I (Figs. 2B–2D) but also that of the degree of linear polarization p (Figs. 2E–2G) of light from the overcast sky has nearly a rotational symmetry. We also obtained that p increases from the zenith toward the horizon, although its wavelength-dependent maximal values remain low ($\leq 4-16\%$). Most important, we found that the pattern of the angle of polarization α of the overcast sky (Figs. 2H-2J and 3) is not only mirror symmetric (with a symmetry axis coinciding with the solar–antisolar meridian), but it is qualitatively the same as that of the clear sky (Figs. 1H–1J). This is a surprising result, because it was a logical assumption that the direction of polarization of light from the overcast sky changes randomly in space and time due to the strong multiple scattering on the particles (ice crystals or water droplets) of thick clouds. Our measurements prove that this is not the case. In the case of a cloudless sky, Rayleigh scattering is definitely the process that explains the direction of polarization. However, in the case of a cloudy sky, the chance that a photon is scattered by a cloud particle is much larger than it is being scattered by a Rayleigh scatterer. Therefore the direction of polarization of cloudlight is determined by scattering on cloud particles themselves.

The rotation of the pattern of the angle of polarization α between scenes S1, S2, and S3 in Fig. 3 is mainly due to the rotation of the icebreaker ship. All three measurements were performed at one of the numerous ice stations of the Beringia 2005 expedition, where the ship stopped

for a few hours on the Arctic Ocean so that the oceanographers could take different measurements. During this period the solar position as well as the direction of the ship's axis changed, the latter because of a slight turning of the icebreaker's body in water. Thus, although our polarimeter was set up at the same place on board (see the contour of the ship's bridge and tower at the same position in pictures S1, S2, and S3 of Fig. 3), the celestial polarization pattern has been rotated relative to the ship. On the other hand, the slight rotation of the α pattern between scenes S6 and S7 (where the polarimetric measurements were done on the Arctic ice cover at a fixed position) is due to the small change of the solar azimuth direction.

We admit that during the evaluation of our polarization measurements sometimes an unfortunate artifact occurred: the α pattern between two subsequent celestial scenes slightly rotated within some minutes. This rotation could not be explained by the small change of the solar azimuth during some minutes. As described in detail by Gál *et al.* [4], our imaging polarimetry is based on three polarization pictures (belonging to three different directions of the transmission axis of the built-in rotatable linear polarizer) recorded by a photo emulsion (roll film). After the chemical development of this photo emulsion, the obtained color dias were framed and scanned, and finally the resulting digitized polarization pictures were evaluated by a computer program. During the evaluation of these dia slides we experienced that smaller or larger rotations of the celestial α pattern can be induced if one of the three polarization pictures is scanned with slightly lower or higher radiance. Under ideal conditions all three polarization pictures should be taken with the same aperture and time of exposure (in the field), and they should be scanned with the same illumination and speed of the scanner (in the laboratory). However, some tiny differences in these recording parameters are always inevitable (e.g., the mechanical shutter of the photographic camera cannot ensure exactly the same time of exposure, and/or the scanner cannot run with exactly the same scanning speed and/or illumination for all three polarization pictures). The effect of this can be demonstrated in such a way as if the radiance values of all pixels in a given polarization picture taken under ideal conditions were multiplied by a factor f, and the values of this factor were different for the three polarization pictures ($f_1 \neq f_2 \neq f_3$). In Fig. 4 the effect of this is demonstrated. Figure 4A shows the color picture of a foggy sky with the visible Sun's disc. If we assume that the corresponding three polarization pictures are ideal, then $f_1=f_2=f_3=1$ would be true (Fig. 4B). Figure 4C demonstrates how this α pattern is rotated if the value of f_1 is increased from 1 to 1.15, for example.

Hence this rotation of the α pattern between subsequent scenes within some minutes is a pity artifact, which may occur only at extremely low degrees of linear polarization $p < 5\%$. Earlier we have already measured the polarization patterns of plenty of different skies (e.g., in Hungary, Switzerland, Turkey, Finland, and Tunisia [4–7,10]), but this rotation artifact never occurred because the average p of skylight was always relatively high ($p \gg 5\%$), as the measured skies were in most of these
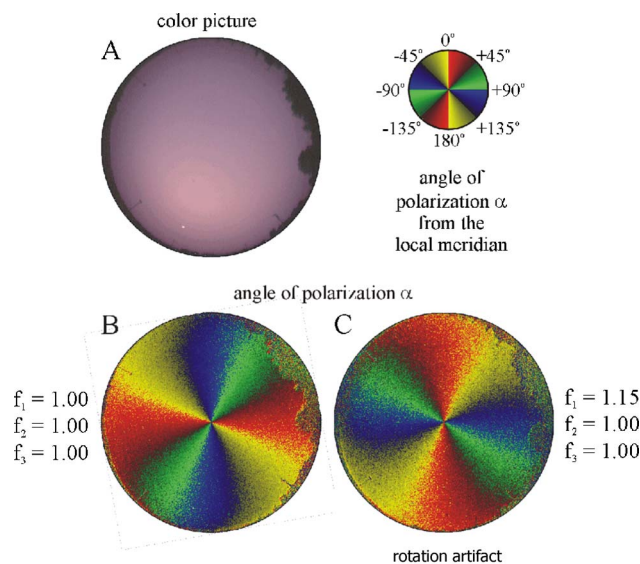
Fig. 4. (Color online) A, Color picture of a foggy sky with the visible Sun's disc. B, Pattern of the angle of polarization α if the radiance values of all pixels in all three polarization pictures (taken with three different directions of the transmission axis of the linear polarizer) are multiplied by factors $f_1 = f_2 = f_3 = 1$. C, The α pattern is artificially rotated if the value of f_1 is increased from 1.00 to 1.15, for example.

cases clear or partly cloudy and in some cases foggy. In the Arctic and during the measurments of overcast skies in the Hungarian town Göd, however, the sky polarization was often so weak ($p < 5\%$) due to the multiple scattering of light on fog and cloud particles that the mentioned rotation artifact could become significant in some cases.

Changing the values of factors f_1, f_2, f_3, the angle of rotation of the celestial α pattern relative to the solar meridian can change almost arbitrarily (e.g., Fig. 4). Unfortunately, this artifact cannot be eliminated because the exact values of f_1, f_2, f_3 are unknown. If the direction of the solar meridian were known, the values of f_1, f_2, f_3 could be reconstructed: one should change these values until the mirror symmetry axis of the celestial α pattern coincides with the solar–antisolar meridian. From the exact point of time and geographical coordinates of a given polarization measurement performed by us the solar position could be calculated. However, in our case the orientation of the polarimeter relative to the magnetic, or geographic North, was unknown because the tripod and its head as well as the housing and body of the polarimeter was slightly ferromagnetic; thus its orientation could not have been determined (nevertheless, the solar–antisolar meridian should coincide with the mirror symmetry axis of a given α pattern). Consequently, in all investigated scenes (Figs. 1–3) the solar position in the circular full-sky patterns was unknown. Thus, the mentioned rotation artifact cannot be compensated. In the future this artifact could be avoided with the use of a digital camera as the detector of the imaging polarimeter. We would like to emphasize, however, that in spite of the occurrence of this rotation artifact, our main conclusion, that the α pattern of overcast skies is similar to that of the clear sky, remains valid henceforward.

Our results presented here together with the findings of Pomozi *et al.* [5], Suhai and Horváth [6], and Hegedüs

et al. [7,8] clearly show that the celestial distribution of the direction of polarization is a very robust pattern being qualitatively always the same under all possible sky conditions. The only qualitative difference among clear, partly cloudy, foggy, smoky, and totally overcast skies is in the degree of linear polarization p: the higher the optical thickness of the non-clear (partly cloudy, smoky, foggy, or overcast) atmosphere, the lower the p value.

The reason for the observed behavior of the angle of polarization $\alpha = 0.5 \times \arctan(U/Q)$ of light from the overcast sky is that α is determined by single scattering. Single scattering by Rayleigh scatterers and by cloud particles (water droplets or ice crystals) produces mainly positive polarization, i.e., perpendicular to the meridian plane of observation [1,9]. The single-scattering process controls the direction of polarization, as well as in the case of multiple scattering, e.g., by clouds. Although the Stokes parameters Q and U become smaller themselves due to multiple scattering, their ratio U/Q remains essentially the same. The degree of linear polarization $p = \sqrt{Q^2 + U^2}/I$, determined by the magnitude of Q and U is more sensitive to the type of particles, especially their size. It could be the task of future research to combine computer simulations of polarized light and our imaging polarimetric measurements to confirm this model. A similar study has already been published for reflected light by Schutgens *et al.* [15].

Some features of the celestial polarization patterns measured by us in the high Arctic and Hungary are the consequence of the high albedo of the ice/snow that covered both the Arctic Ocean and the ground in Hungary where our sky polarization measurements were taken. The albedo of snow is about 90% in the visible and near infrared parts of the spectrum and approaches 98% in the ultraviolet [1]. Coulson ([1], pp. 293–300) reviewed the earlier measurements of skylight polarization over snow surfaces at high absolute latitudes ($77° - 90°$) and low solar elevations ($10° - 14°$). Bullrich *et al.* [16] measured the sky polarization in North Greenland, while Coulson [1] took measurements above snow-covered terrains of the Antarctic continent:

1. One of the characteristics of sky polarization over extended snow surfaces is that the maximum p_{max} of the degree of linear polarization p is low (30–60%) relative to that of the normal clear sky (50–85%). This is due to the high reflectivity of the snow surface and the nearly unpolarized character of the snow-reflected light. The snow reflects a large amount of approximately unpolarized light into the atmosphere at all wavelengths. When backscattered from the atmosphere toward the Earth's surface, this snow-reflected unpolarized light reduces considerably the net p of skylight in every spectral range.

2. A further characteristic of skylight polarization over snow surfaces is that p_{max} increases slightly with increasing wavelength because of the slight decrease of snow reflectivity with increasing wavelength. Thus, at longer wavelengths a lesser amount of snow-reflected light dilutes the linearly polarized skylight than at shorter wavelengths.

3. The third characteristic of sky polarization above snow surfaces is that the regions of negative polarization

(characterized by angles of polarization $-45° \leq \alpha \leq +45°$ measured from the local meridian) near the Sun and anti-Sun is larger at the shorter wavelengths than at the longer ones. This is due to the introduction of a small amount of positive polarization into the skylight by the reflection of the snow surface at longer wavelengths.

We experienced that all polarization patterns measured by us under clear and overcast skies above ice/snow-covered surfaces both in the high Arctic and Hungary bear the characteristics listed in the above points.

During the Beringia 2005 expedition to the North Pole region in all the measurements of overcast skies we found that the solar elevation angle ϵ was not higher than 7.3° (Table 1). The measured polarization patterns of Arctic overcast skies were compared with those of overcast skies above different terrains with or without snow cover (Fig. 3, Tables 1 and 2). Such a comparison can be made only if the solar elevations are similar. This is the reason why ϵ of our observations was usually so small (see scenes S9, S11, S12, S14, and S15). Note, however, that in two cases (scenes S10 and S13) we measured the celestial α pattern approximately at noon, when ϵ was nearly maximal. Thus we can conclude that the α pattern of overcast skies is similar to that of the clear sky for both low and high solar elevations.

B. Consequences for Compass Orientation in Polarization-Sensitive Animals

The fact that the celestial α pattern is so robust, being qualitatively the same under all sky conditions, is of great importance for the orientation of polarization-sensitive animals based on skylight polarization: if the degree of linear polarization p of skylight is higher than the threshold p^* of the polarization sensitivity of animals, then their orientation can be governed by the celestial angle of polarization α, from the pattern of which the direction of the solar meridian can be determined if the Sun is occluded by fog, smoke, clouds, or canopy. Although p of light from the overcast skies S1–S15 studied by us was not higher than 16%, the threshold of polarization sensitivity in field crickets (*Gryllus campestris*) and honey bees (*Apis mellifera*), for example, is $p^* = 5\%$ and 10% [10]. This means that these animals could use the celestial α pattern for navigation even under totally overcast conditions. In the future it would be worth testing this prediction, which is atmospheric optically supported by our results presented in this work.

Our findings suggest that despite what has previously been thought, animals using the skylight polarization pattern for compass orientation and compass calibration should be able to use this cue also under totally overcast skies, if they can perceive light with low degrees of linear polarization ($\leq 16\%$ in our study). Experiments with migratory thrushes in North America show that these birds calibrate their magnetic compass on the basis of natural twilight cues at least once per day during migration [17]. Recently it has been demonstrated that Savannah sparrows (*Passerculus sandwichensis*), also a North American songbird known to favor twilight polarization cues before stellar and magnetic cues at sunset [18], use the polarization pattern of the lower part of the sky to calibrate their

magnetic compass [19]. It is interesting to note that in our measurements the highest degree of linear polarization under overcast skies was found near the horizon, suggesting that taking notice of this part of the sky when calibrating the magnetic compass could be a wise strategy by the birds mentioned; in fact, during some circumstances it could be the only part of the sky where the skylight polarization information could be assessed by them.

REFERENCES

1. K. L. Coulson, *Polarization and Intensity of Light in the Atmosphere* (A. Deepak, 1988).
2. K. J. Voss and Y. Liu, "Polarized radiance distribution measurements of skylight. I. System description and characterization," Appl. Opt. **36**, 6083–6094 (1997).
3. J. A. North and M. J. Duggin, "Stokes vector imaging of the polarized sky-dome," Appl. Opt. **36**, 723–730 (1997).
4. J. Gál, G. Horváth, V. B. Meyer-Rochow, and R. Wehner, "Polarization patterns of the summer sky and its neutral points measured by full-sky imaging polarimetry in Finnish Lapland north of the Arctic Circle," Proc. R. Soc. London, Ser. A **457**, 1385–1399 (2001).
5. I. Pomozi, G. Horváth, and R. Wehner, "How the clear-sky angle of polarization pattern continues underneath clouds: full-sky measurements and implications for animal orientation," J. Exp. Biol. **204**, 2933–2942 (2001).
6. B. Suhai and G. Horváth, "How well does the Rayleigh model describe the E-vector distribution of skylight in clear and cloudy conditions? A full-sky polarimetric study," J. Opt. Soc. Am. A **21**, 1669–1676 (2004).
7. R. Hegedüs, S. Åkesson, R. Wehner, and G. Horváth, "Could Vikings have navigated under foggy and cloudy conditions by skylight polarization? On the atmospheric optical prerequisites of polarimetric Viking navigation under foggy and cloudy skies," Proc. R. Soc. London, Ser. A **463**, 1081–1095 (2007).
8. R. Hegedüs, S. Åkesson, and G. Horváth, "Anomalous celestial polarization caused by forest fire smoke: why do some insects become visually disoriented under smoky skies?" Appl. Opt. **46**, 2717–2726 (2007).
9. G. P. Können, *Polarized Light in Nature* (Cambridge U. Press, l985).
10. G. Horváth and D. Varjú, *Polarized Light in Animal Vision—Polarization Patterns in Nature* (Springer-Verlag, 2003).
11. K. L. Coulson, "On the solar radiation field in a polluted atmosphere," J. Quant. Spectrosc. Radiat. Transf. **2**, 739–755 (1971).
12. M. L. Brines and J. L. Gould, "Skylight polarization patterns and animal orientation," J. Exp. Biol. **96**, 69–91 (1982).
13. J. W. Strutt (Lord Rayleigh), "On the light from the sky, its polarisation and colour. I," Philos. Mag. **41**, 107–120 (1871).
14. J. W. Strutt (Lord Rayleigh), "On the light from the sky, its polarisation and colour. II," Philos. Mag. **41**, 274–279 (1871).

15. N. A. J. Schutgens, L. G. Tilstra, P. Stammes, and F.-M. Bréon, "On the relationship between Stokes parameters Q and U of atmospheric ultraviolet/visible/near-infrared radiation," J. Geophys. Res. **109**, D09205, doi: 10.1029/2003JD004081 (2004).
16. K. Bullrich, R. Eiden, and W. Nowak, "Sky radiation, polarization, and twilight radiation in Greenland," Pure Appl. Geophys. **64**, 220–242 (1966).
17. W. W. Cochran, H. Mouritsen, and M. Wikelski, "Migrating songbirds recalibrate their magnetic compass daily from twilight cues," Science **304**, 405–408 (2004).
18. K. P. Able and M. Able, "The flexible migratory orientation system of the Savannah sparrow (*Passerculus sandwichensis*)," J. Exp. Biol. **199**, 3–8 (1996).
19. R. Muheim, J. B. Phillips, and S. Åkesson, "Polarized light cues underlie compass calibration in migratory songbirds," Science **313**, 837–839 (2006).